Optical Coherence Tomography:

Applications to the characterization of regional material properties in murine models of aortic dissections

Stéphane Avril

Introduction to

OCT/DVC

Optical Coherence Tomography (OCT)

avril@emse.fr

Optical Coherence Tomography

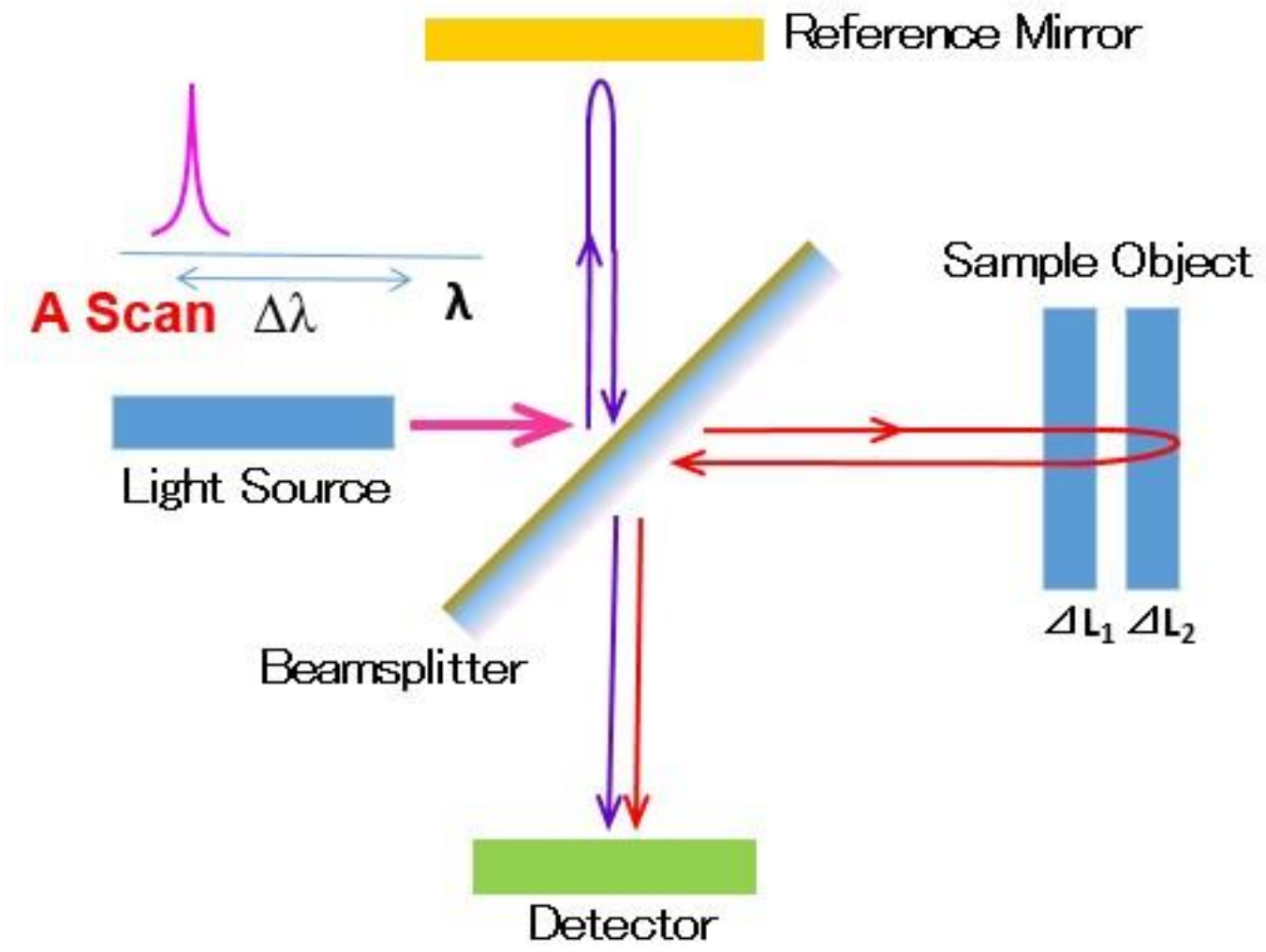

Spectral OCT

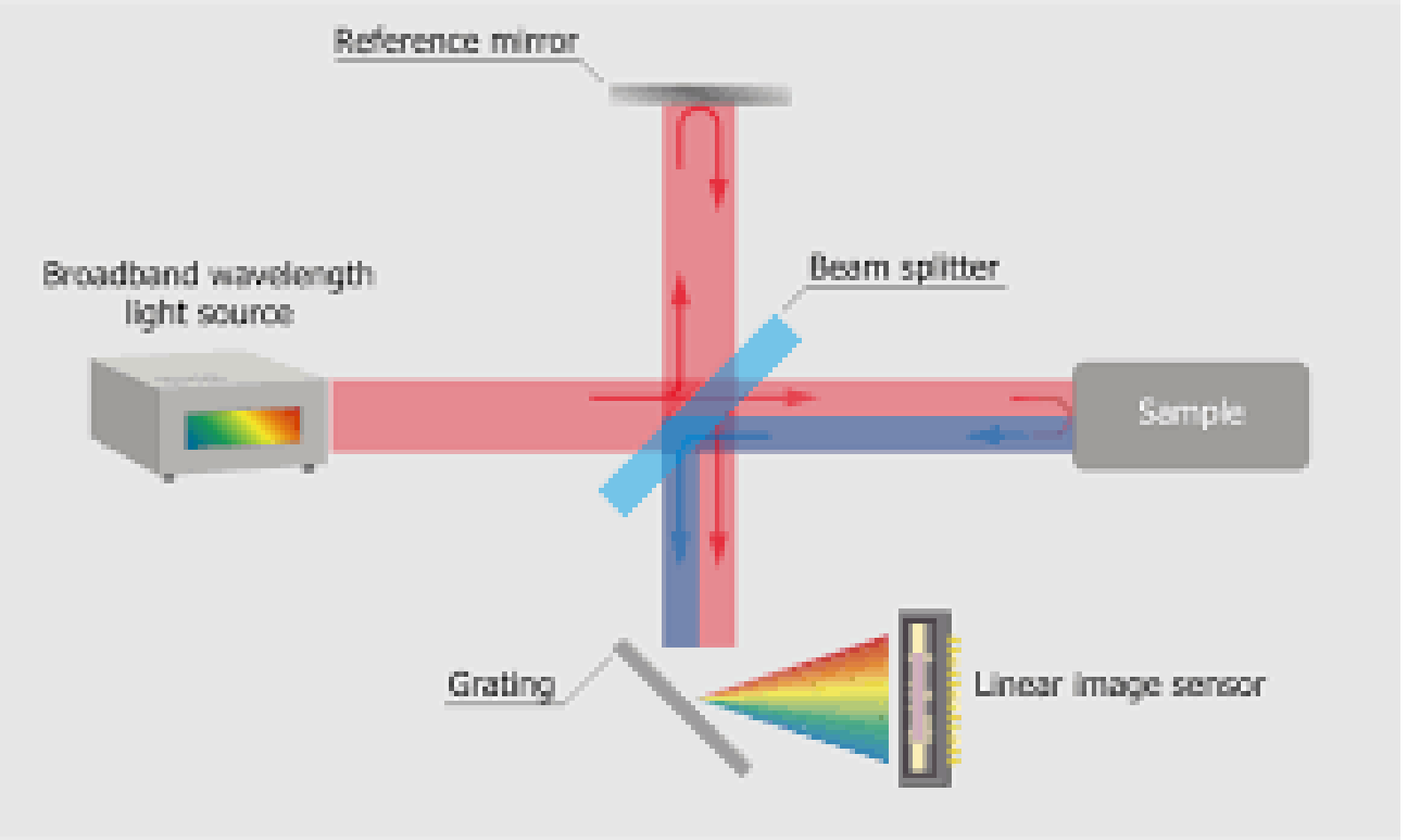

Medical applications of OCT

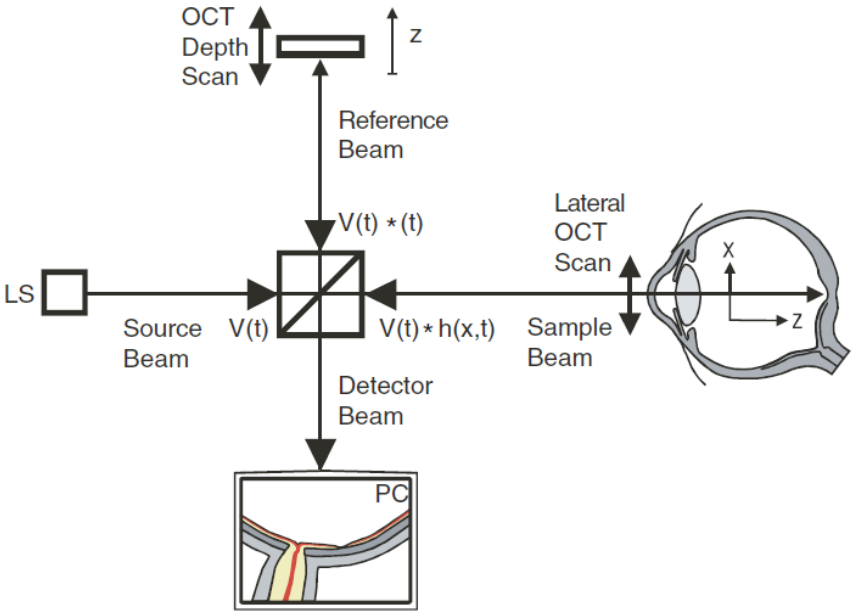

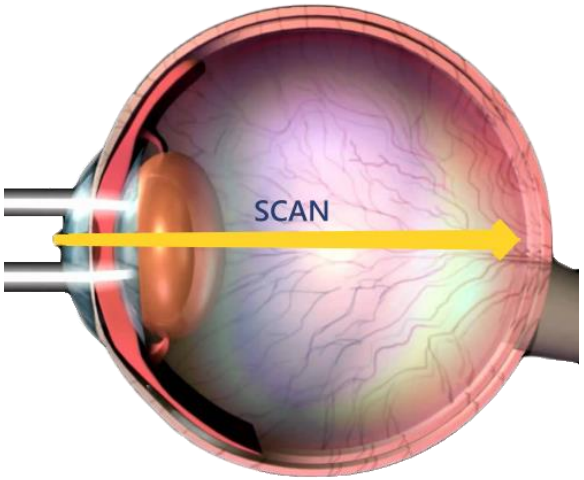

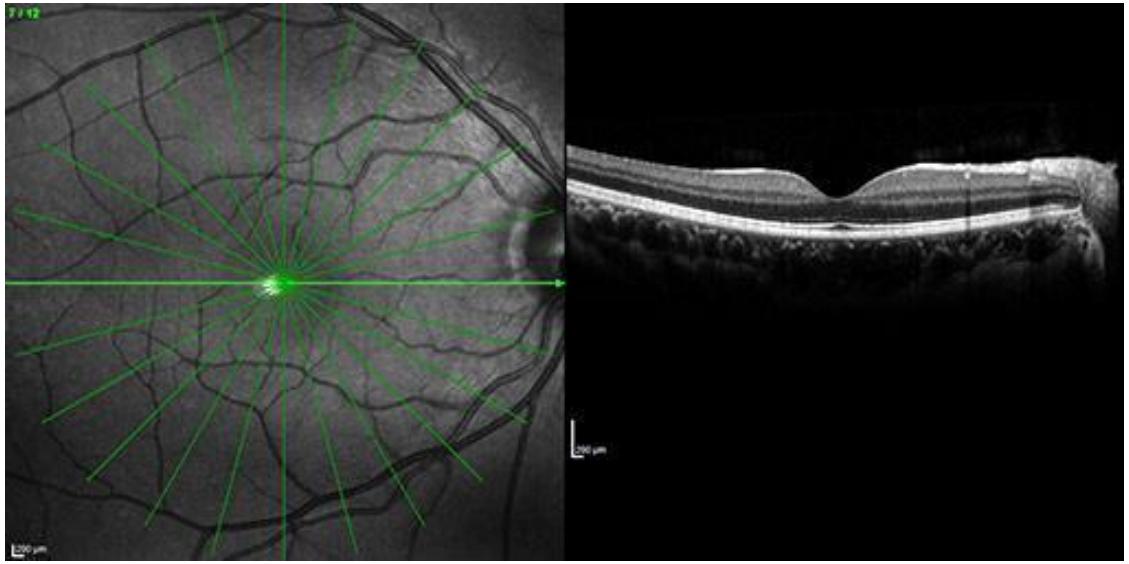

Extension of OCT to image arteries *in vitro*

Frontiers in Mechanical Engineering, 2018, 4, 3

Acta Biomaterialia, 2020, 102, 127-137

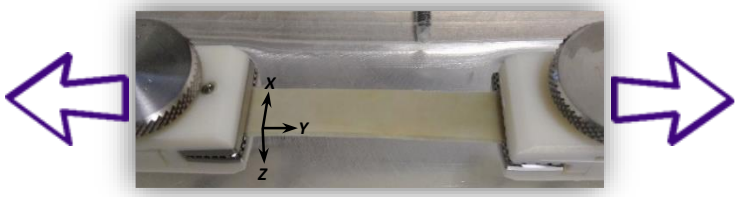

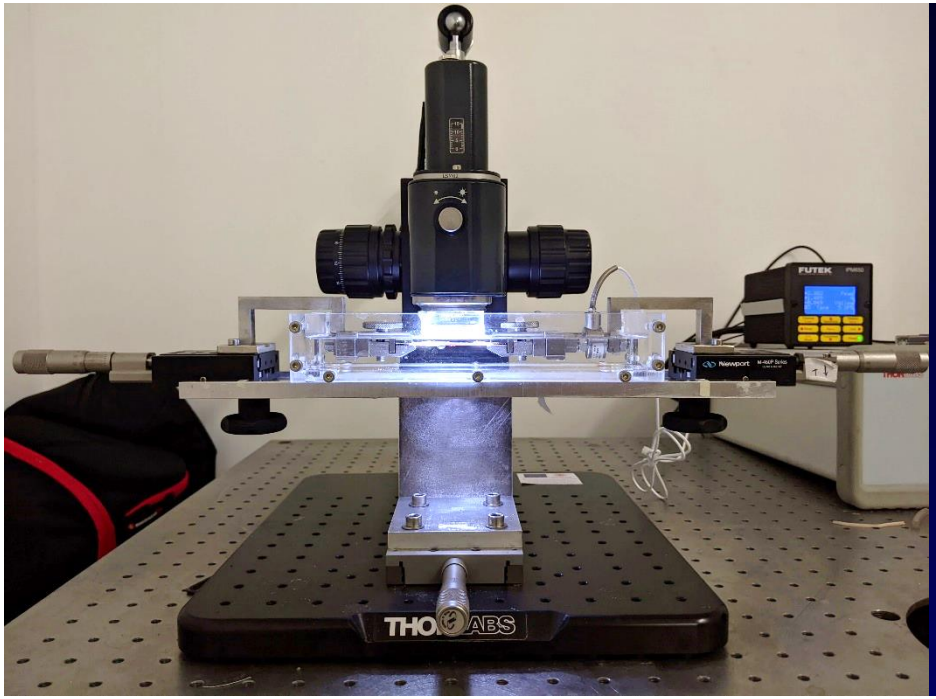

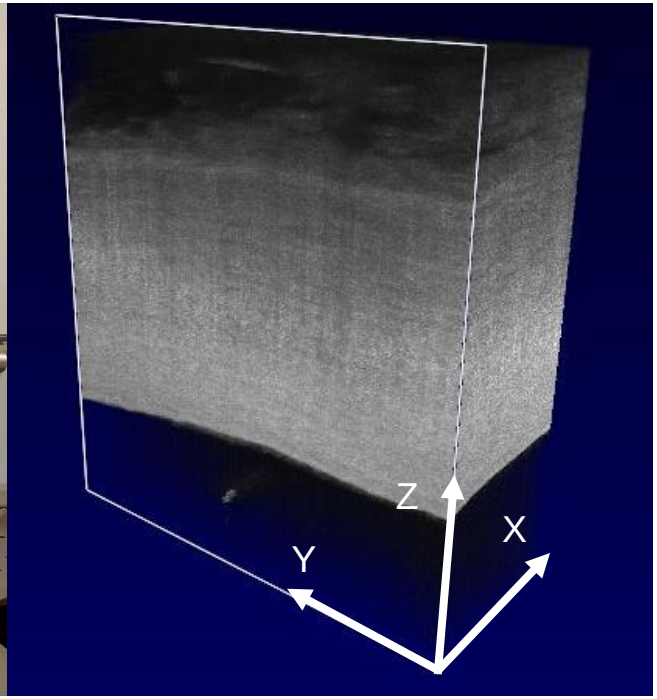

avril@emse.fr

MINES Saint-Étienne

Extension of OCT to image arteries *in vitro*

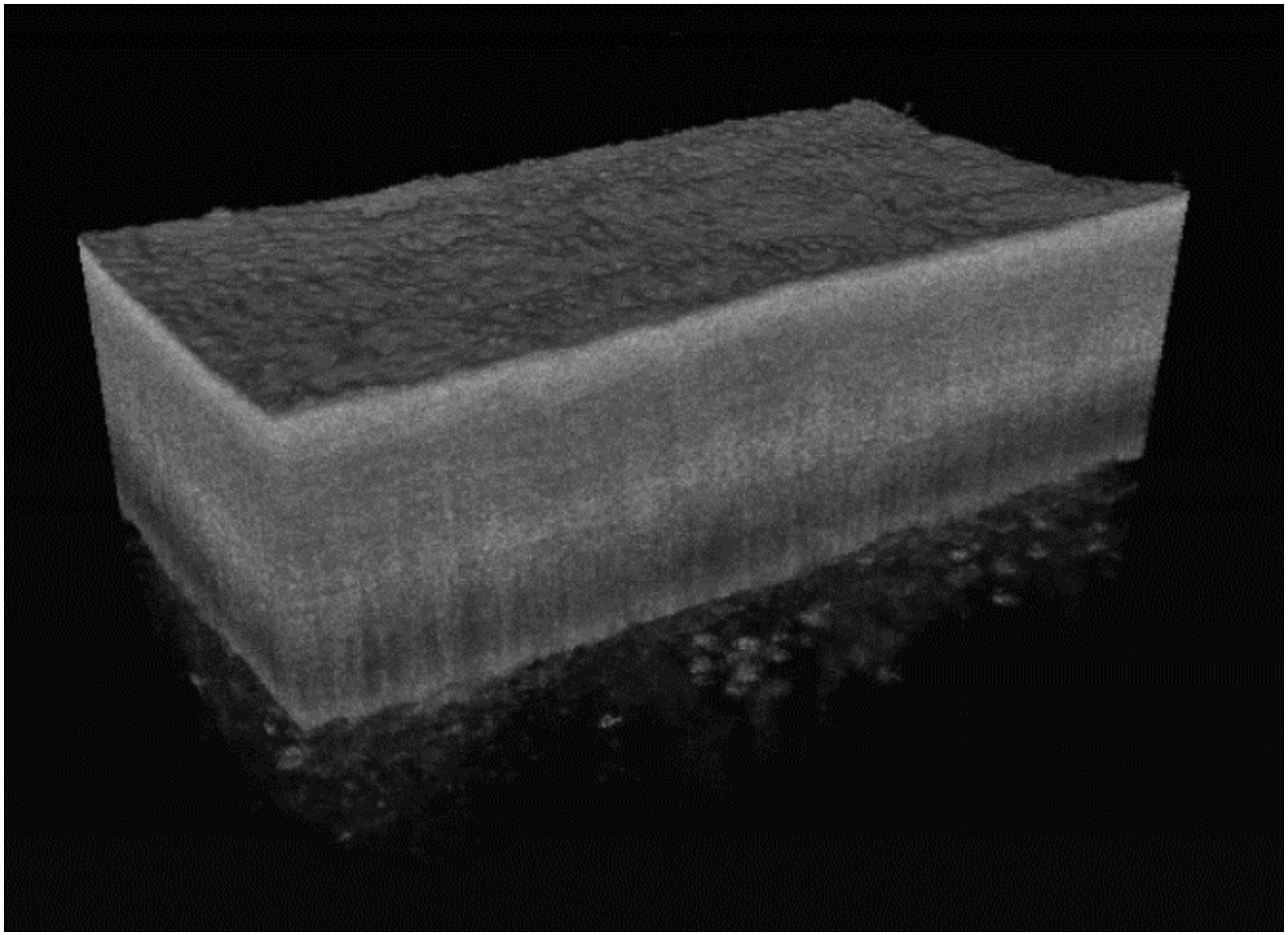

avril@emse.fr

Extension of OCT to image arteries *in vitro*

Lane et al, under review (2022)

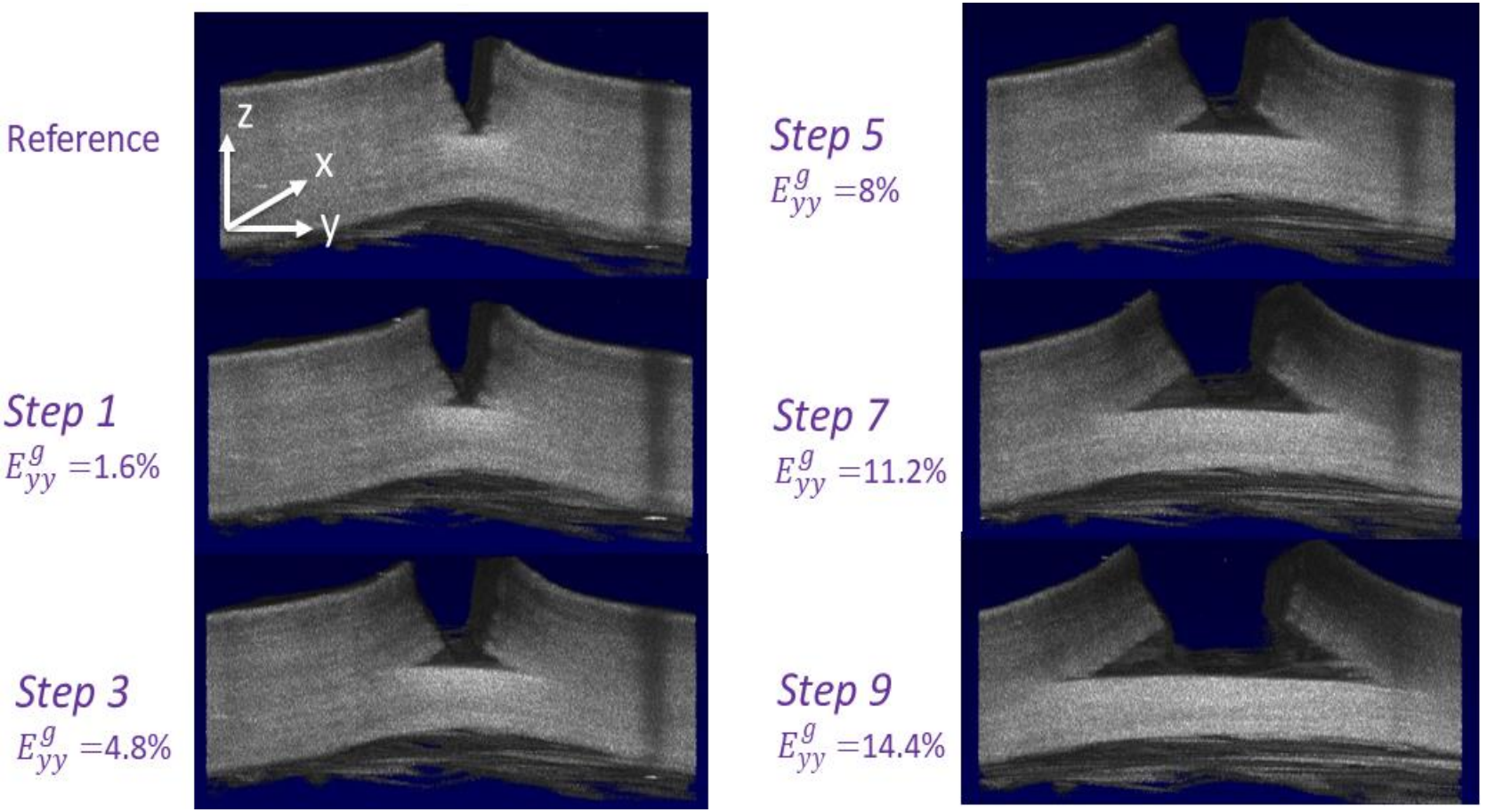

avril@emse.fr

Digital Volume Correlation

- Digital Volume Correlation (DVC) tracks sub-volumes with multiple voxels to measure local displacements within the volume

- Requires unique and random innate pattern within the volume for tracking

- Refractive index of vascular constituents create innate pattern in the OCT images

Digital Volume Correlation

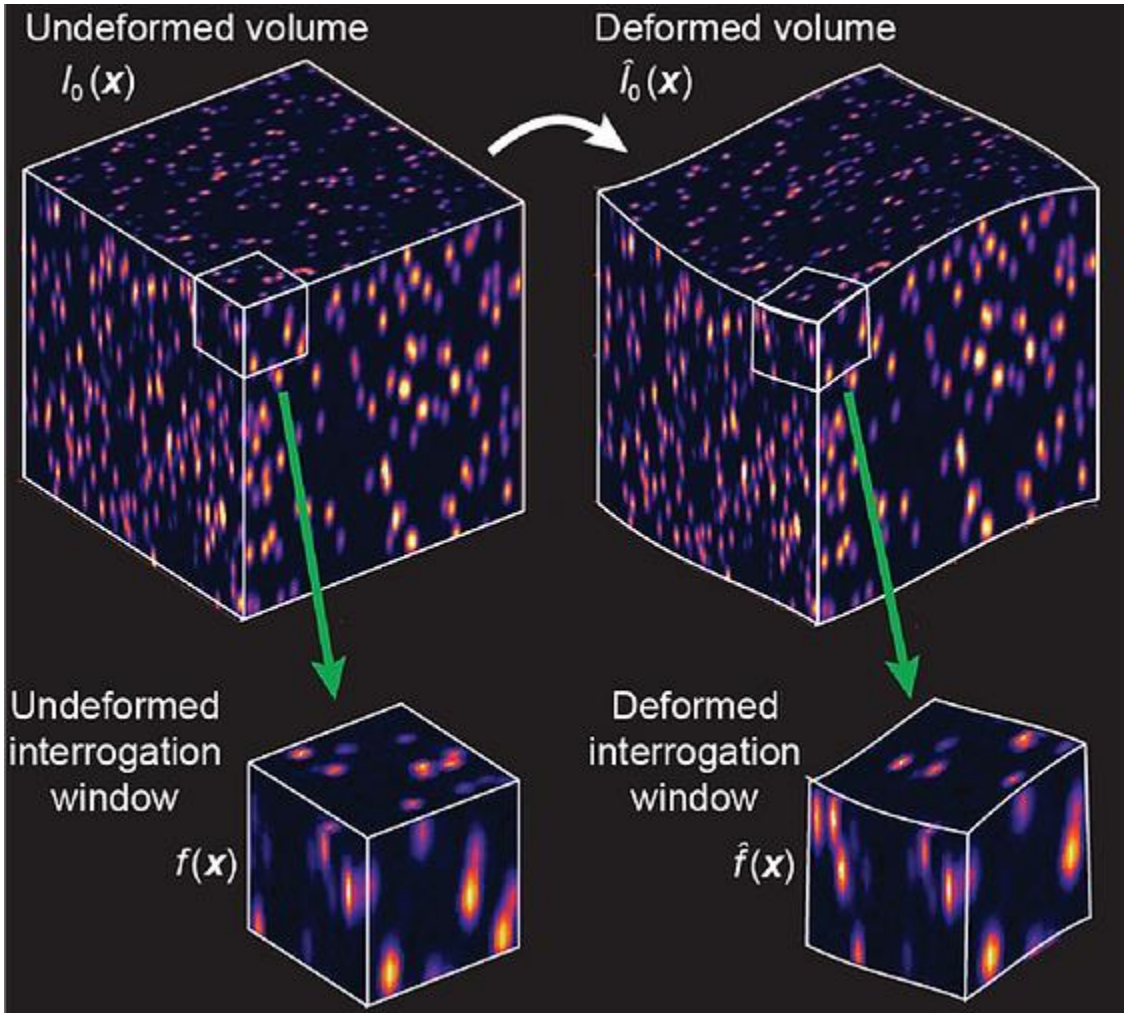

OCT/DVC to test arteries *in vitro*

Acta Biomaterialia, 2020, 102, 127-137

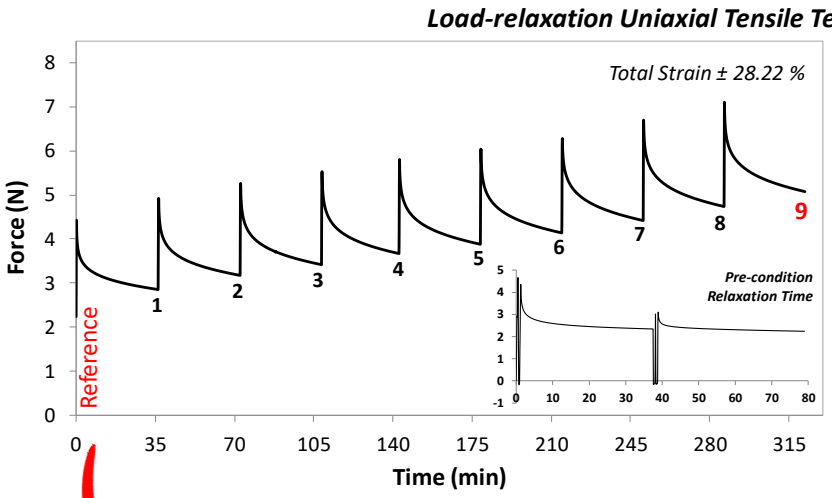

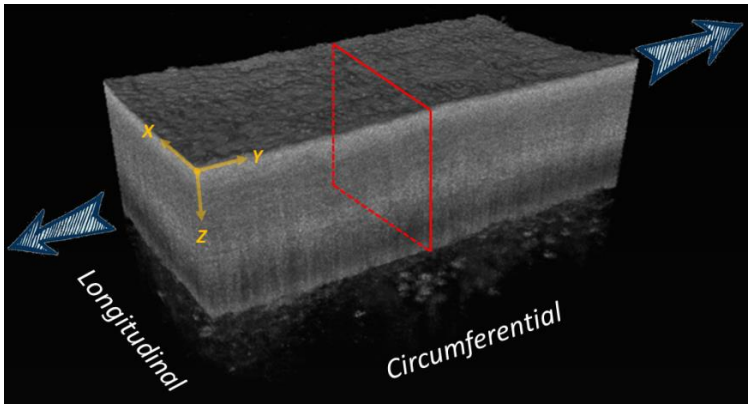

Full-field
Displacement Measurements

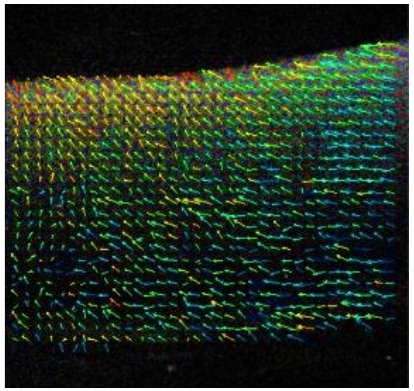

Correlation
(Reference vs Final Loading Stage)

Full-field Strain Measurements – Green-Lagrange Strain Tensor (E_{yy})

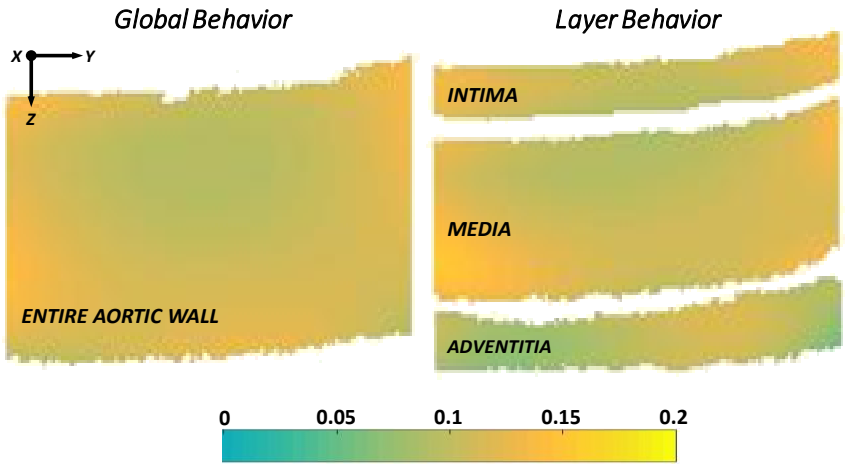

OCT/DVC to test arteries *in vitro*

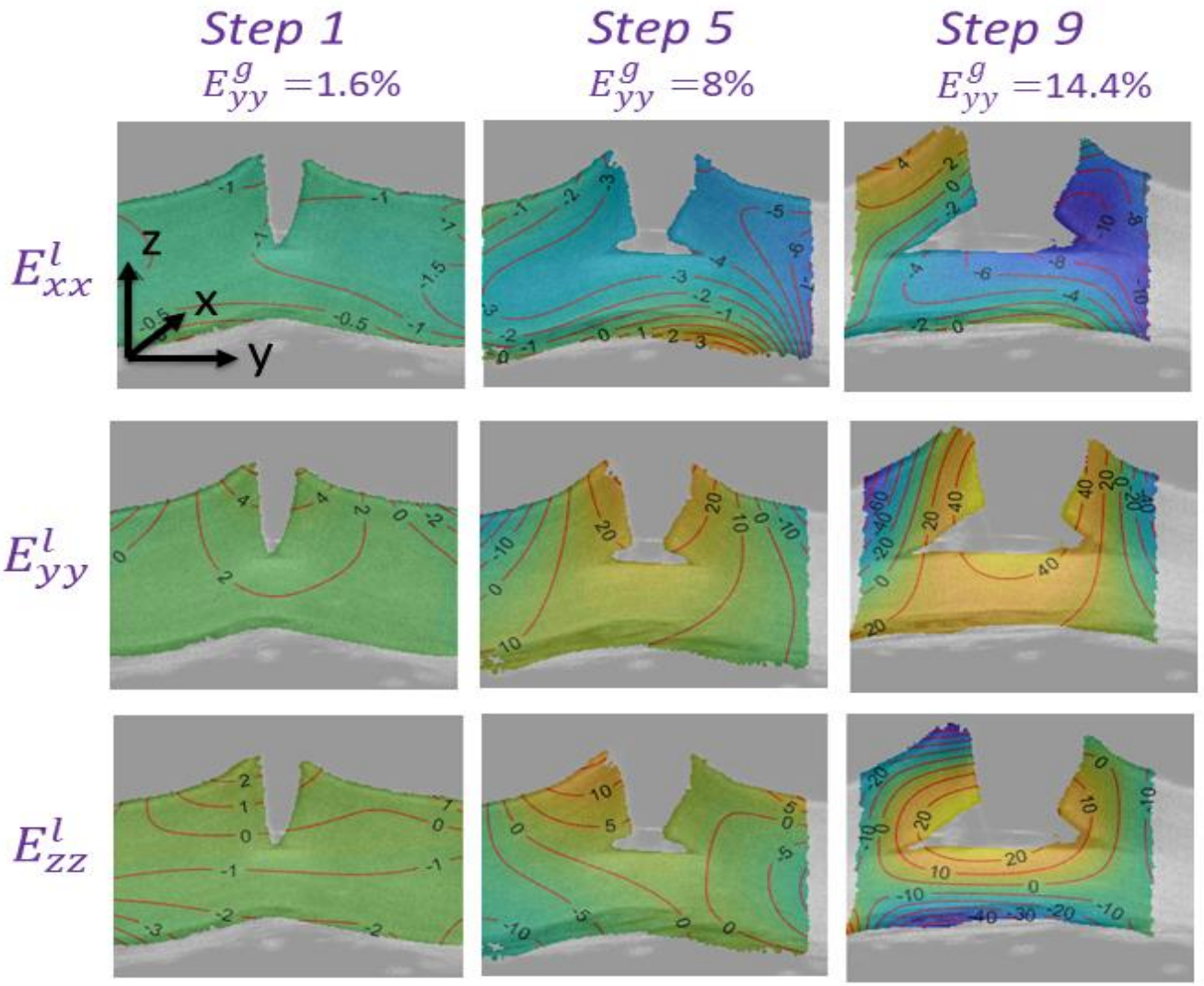

avril@emse.fr

Application to determine structure/function relationships in mice models of dissections

METHODS

APPROACH

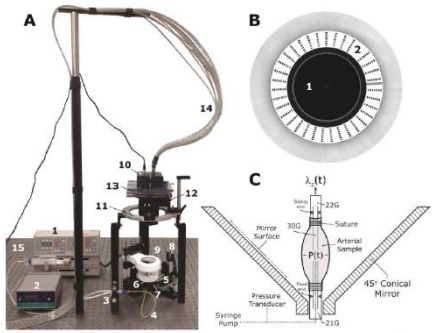

1. **Experiments**
2. Material model
3. Inverse method

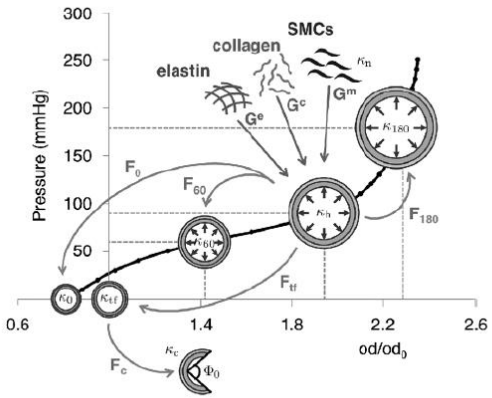

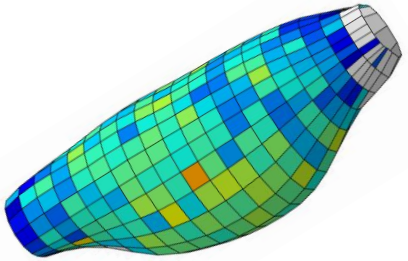

avril@emse.fr

Angiotensin-II Infusion Model of AAD

- Male ApoE $^{-/-}$ mice at 16-20 weeks of age surgically implanted with subcutaneous osmotic pump lateral to dorsal midline at mid-scapular region
- Maintained constant infusion of ANG-II at a rate of 1000 ng/kg/min

Aortic Dissection

Dissecting Aortic Aneurysm

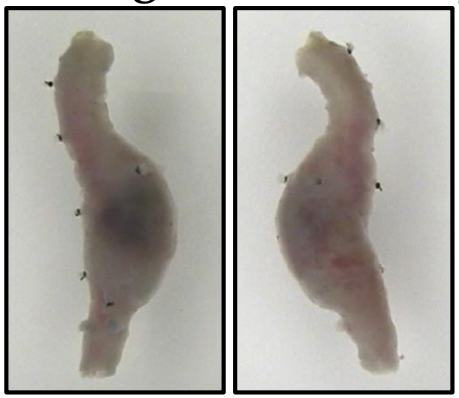

Anterior Posterior

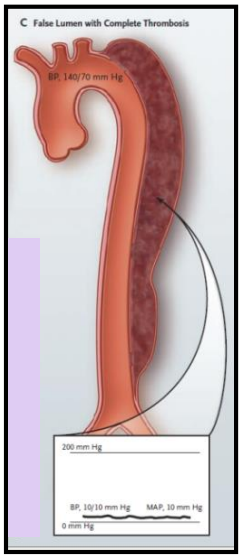

Descending Thoracic

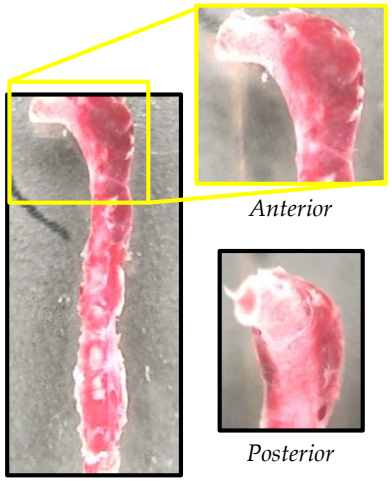

Anterior

Posterior

Suprarenal

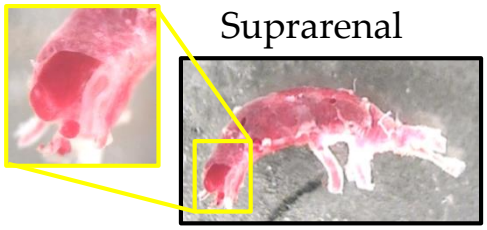

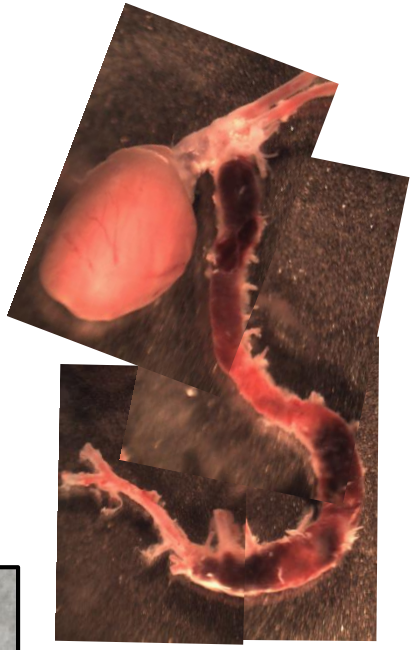

Intact Aorta

Experimental Approach

- **Angiotensin-II Infusion Model of AAD**
- **Timeline**

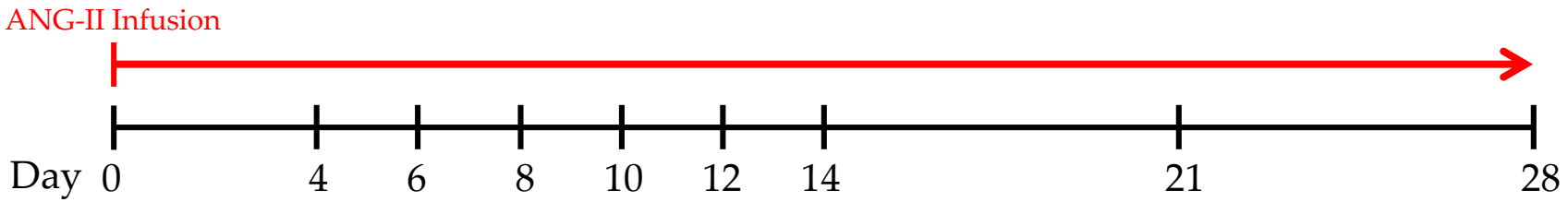

- **Peak in macrophage activity at day 4 with dissection occurring between days 1 and 4 followed by associated remodeling from days 4 to 10.**

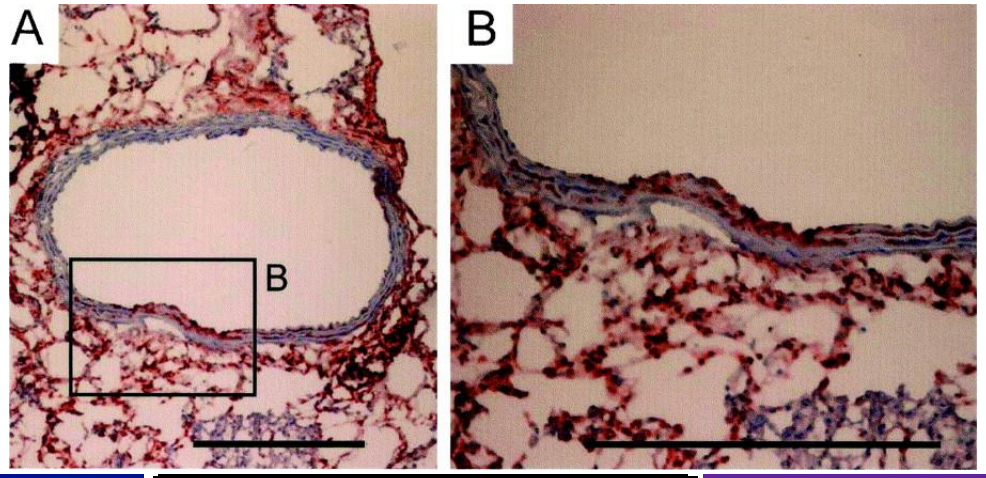

IHC showing medial infiltration of macrophages after 48 hours of treatment

Sarafi et al. (2003)

Material discretization using OCT

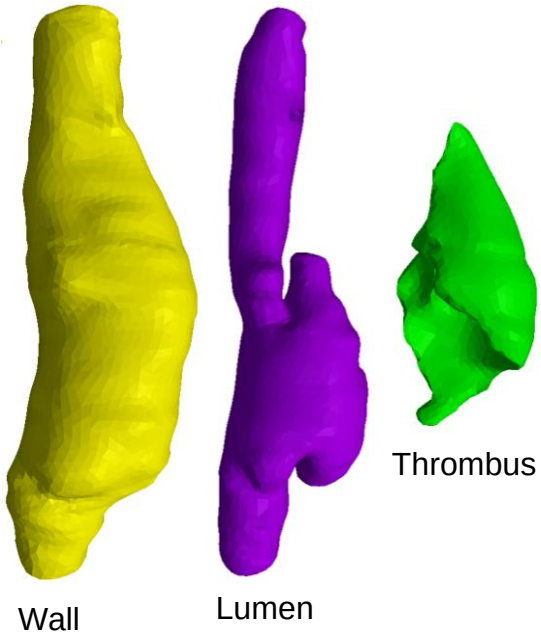

Segmented 3D model:

Clipping planes:

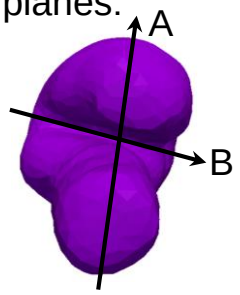

Contours of model through planes A and B:

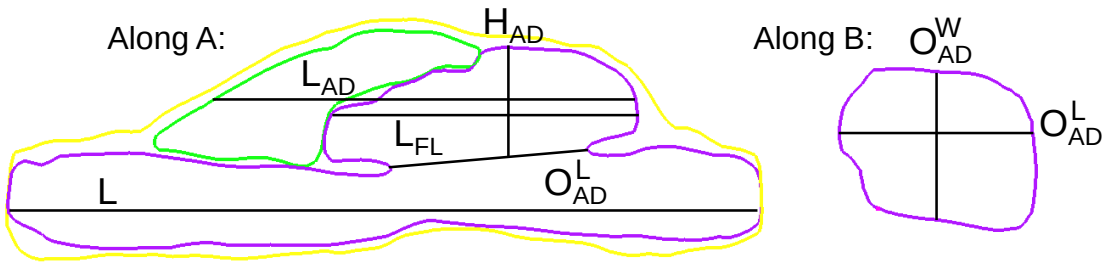

Scientific Reports, 2020, 10(1), 1-23

Full-Field Thickness Estimation using OCT

BMMB, 2019, 18(1), 203–218

Fibulin 4 SMC KO

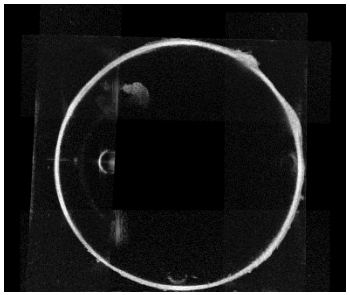

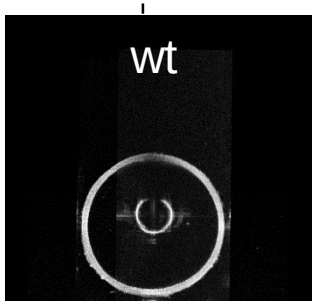

Fibrillin 1 *mgR/mgR*

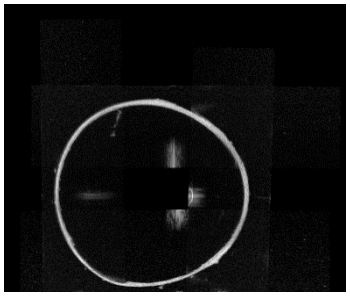

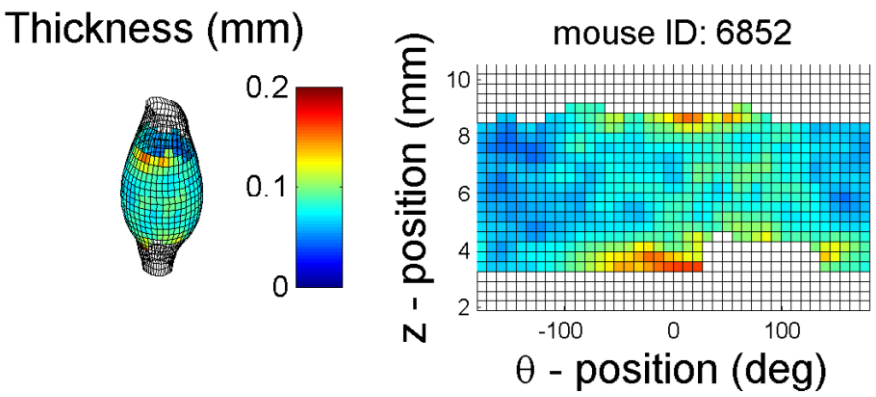

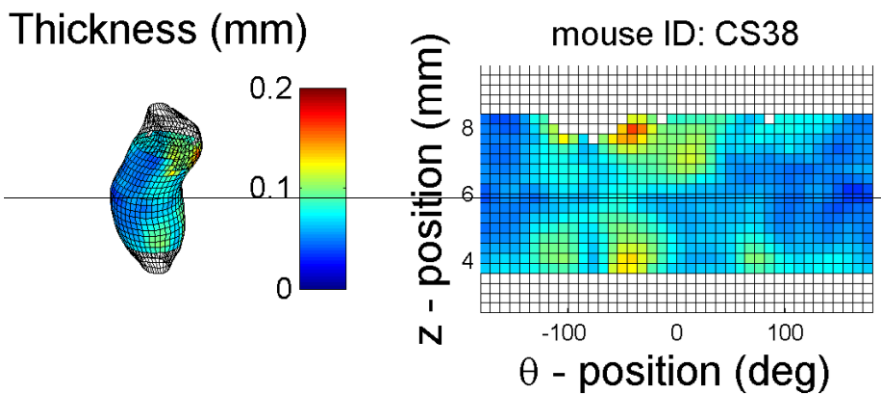

avril@emse.fr

MINES Saint-Étienne

OCT reveals 2 primary types of mural defects in the ATA

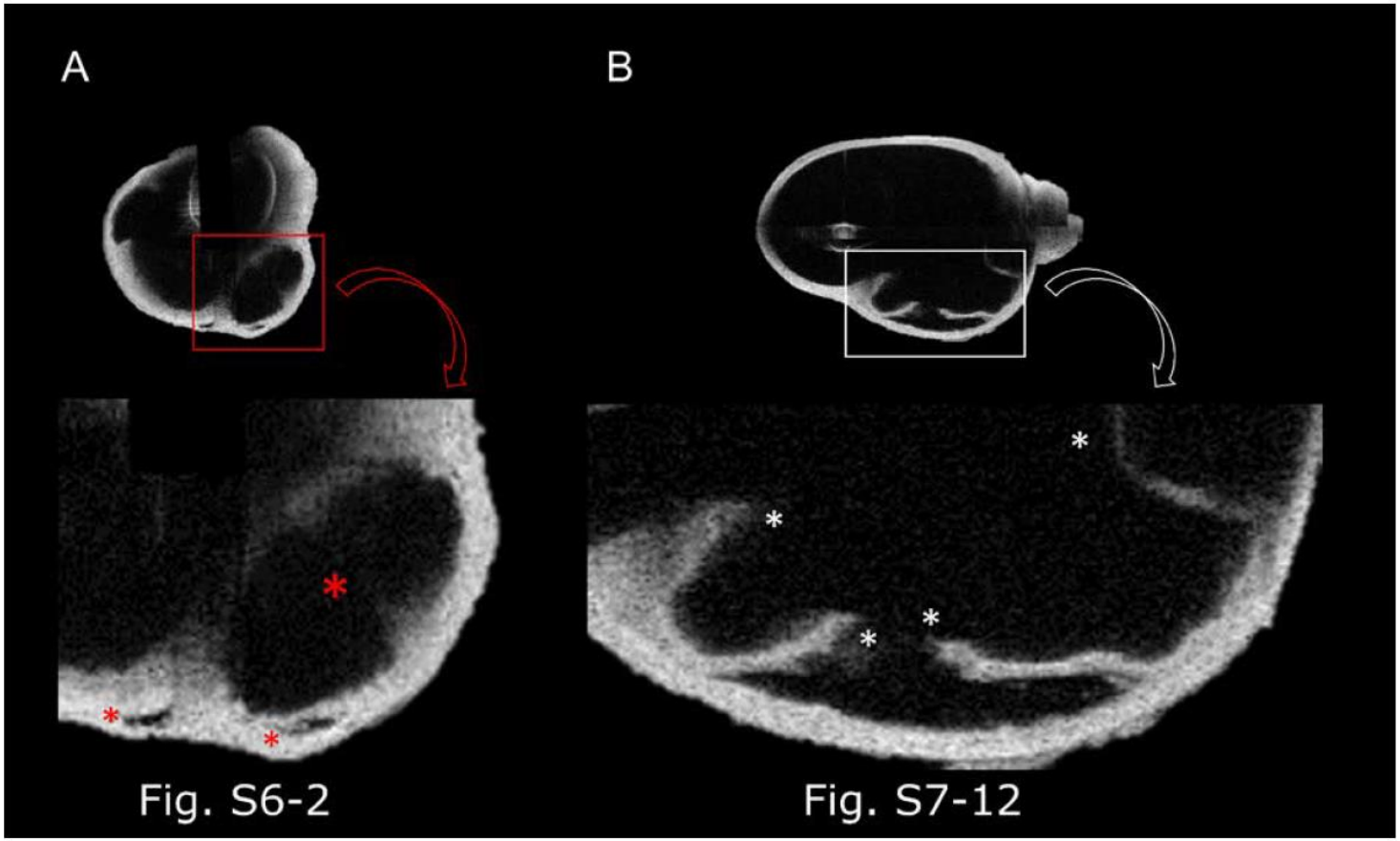

Weiss et al, ATVB, 2022

Thrombus measurements using OCT

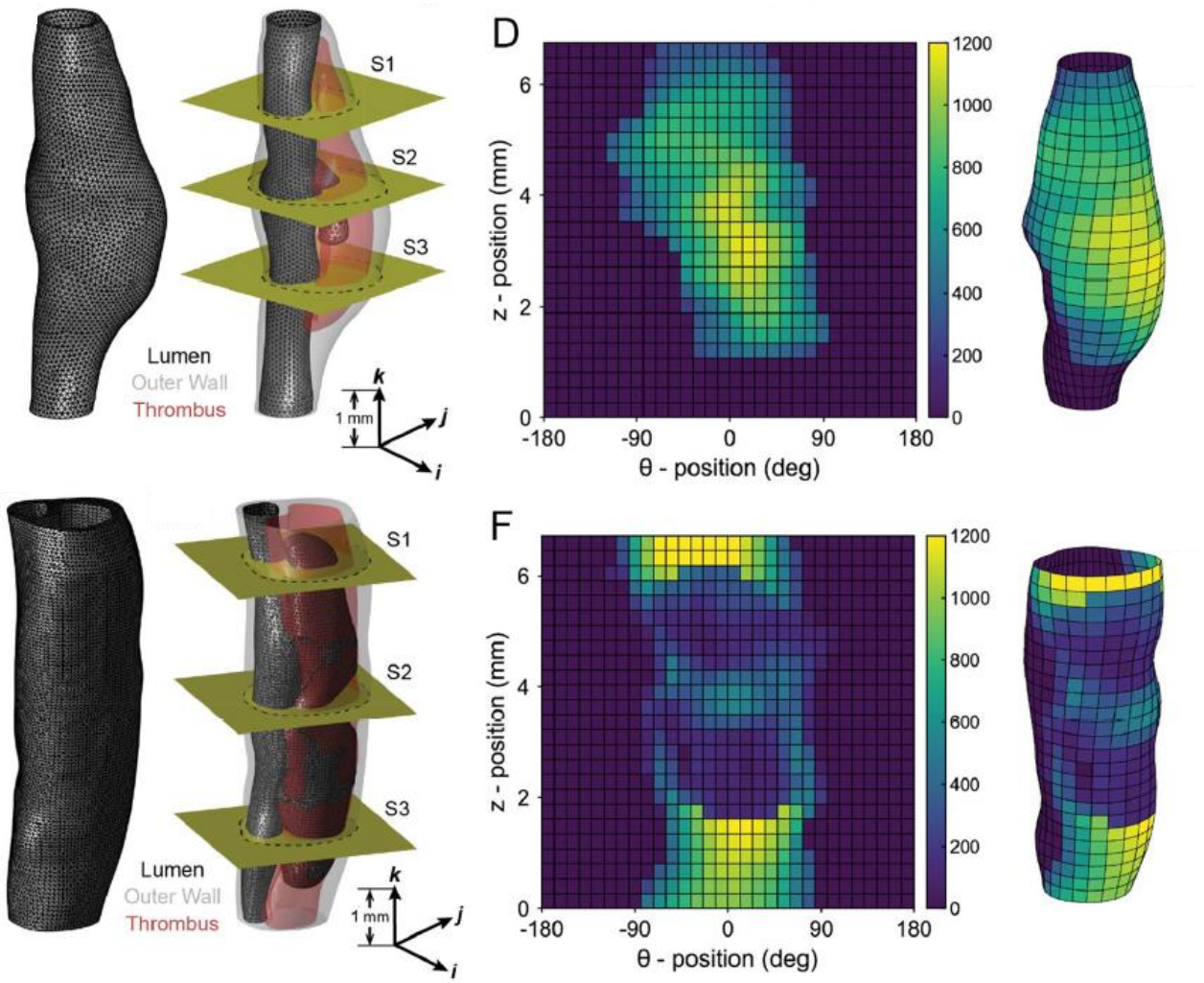

avril@emse.fr

Tension inflation tests

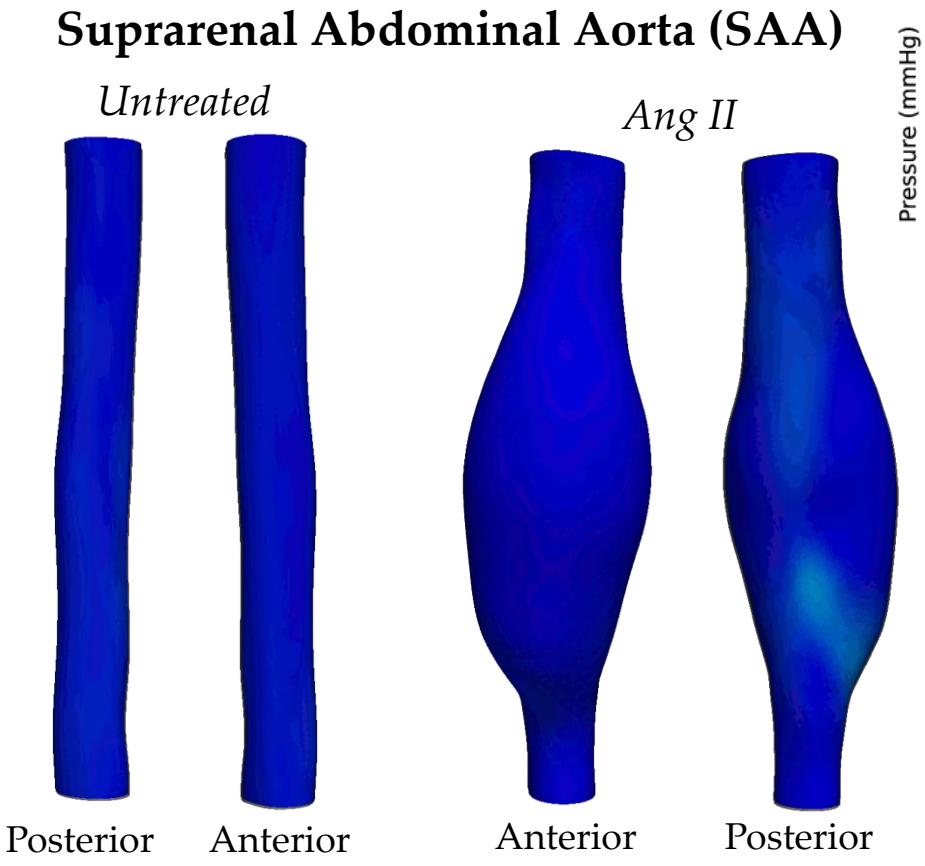

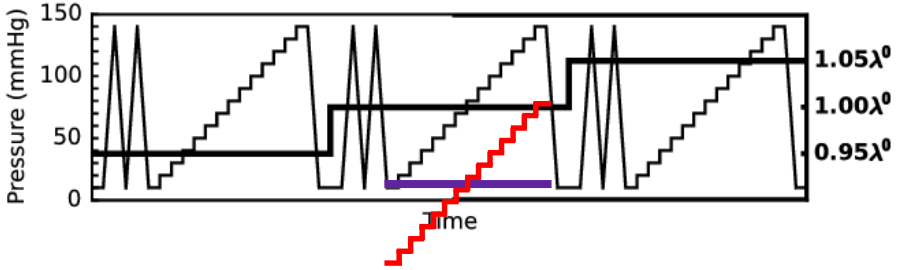

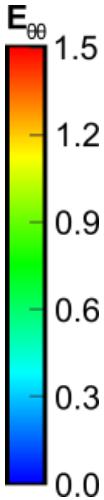

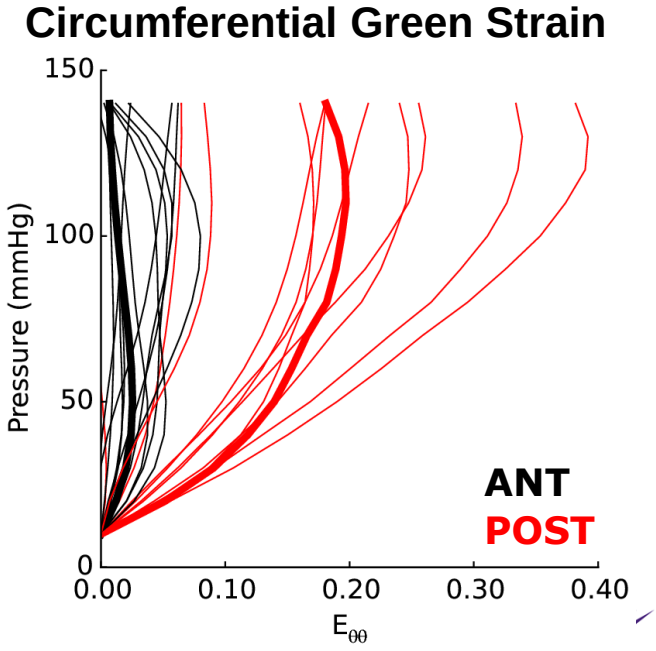

Science Advances, 2020, 6(49), eabd3574.

Measurement of bulk deformation fields by Digital Volume Correlation on OCT images

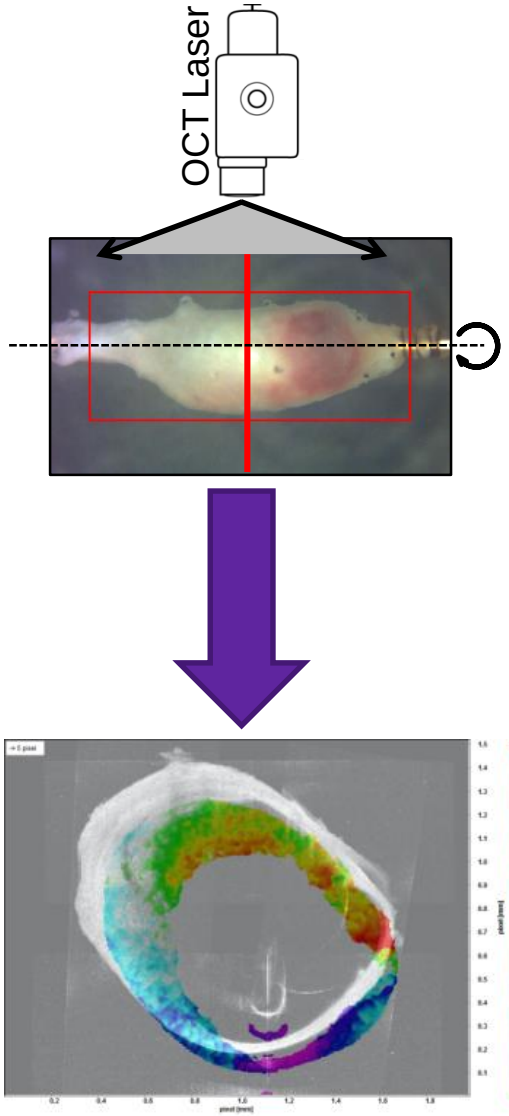

Scientific Reports, 2020, 10(1), 1-23

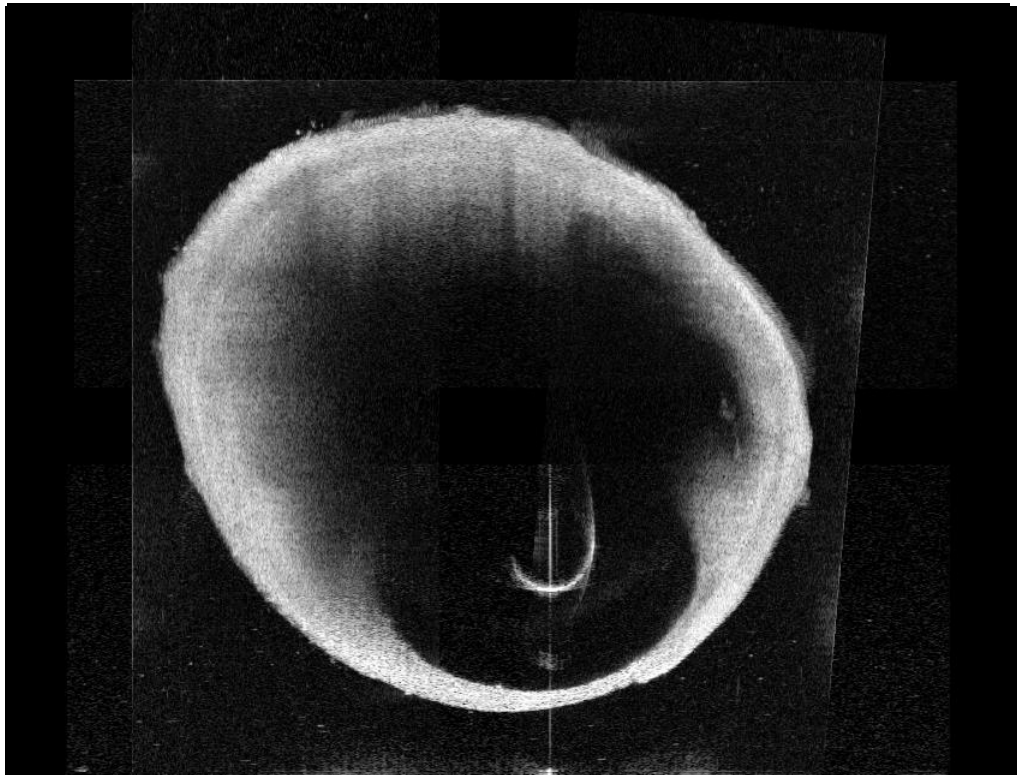

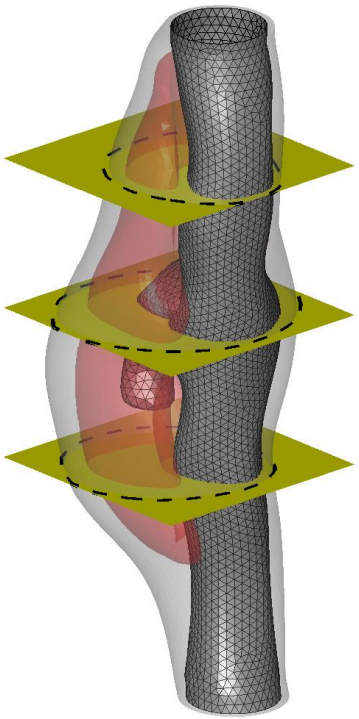

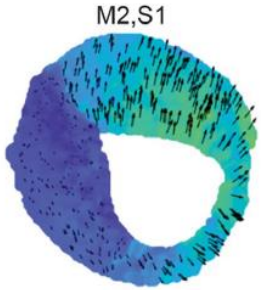
M2,S1

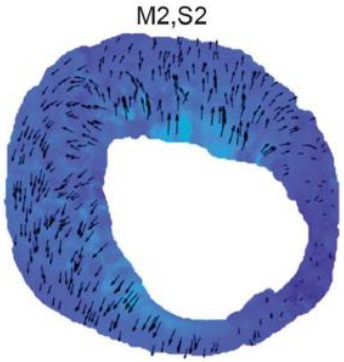
M2,S2

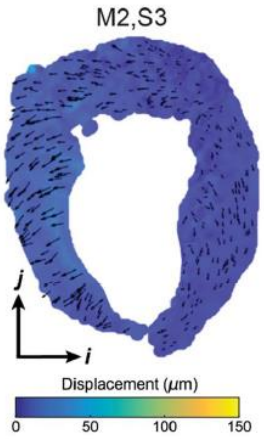
M2,S3
j
i
Displacement (μm)
0
50
100
150


M4,S1

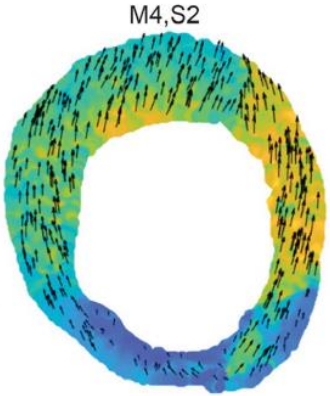
M4,S2

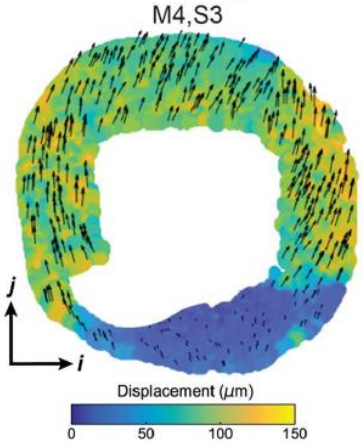
M4,S3
j
i
Displacement (μm)
0
50
100
150

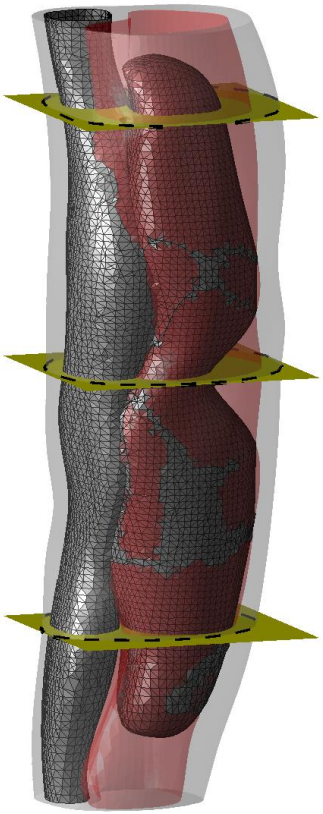

APPROACH

1. Experiments
2. **Material model**
3. Inverse method

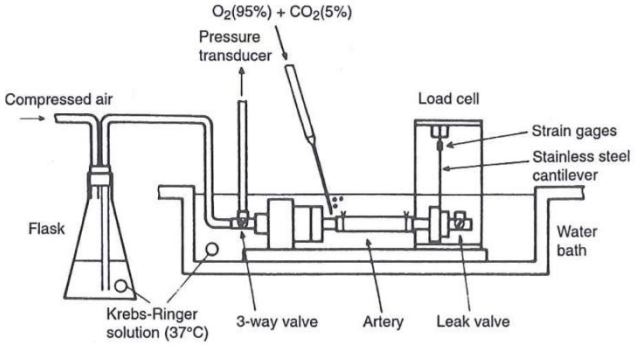

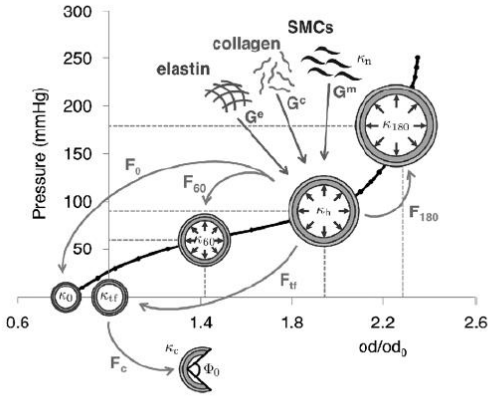

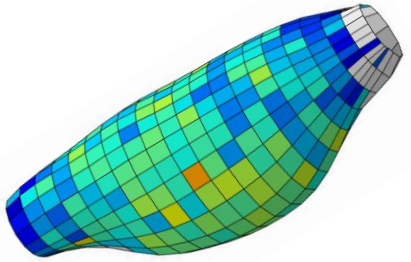

avril@emse.fr

CONSTITUTIVE MODEL

Strain energy functions:

$$W = \phi^{e} W^{e}(\mathbf{F}^{e}) + \phi^{m} W^{m}(\lambda^{m}) + \sum_{j=1}^{4} \phi^{c_j} W^{c_j}(\lambda^{c_j})$$

Ann. Biomed. Eng., **42**(3), pp. 488–502, 2014

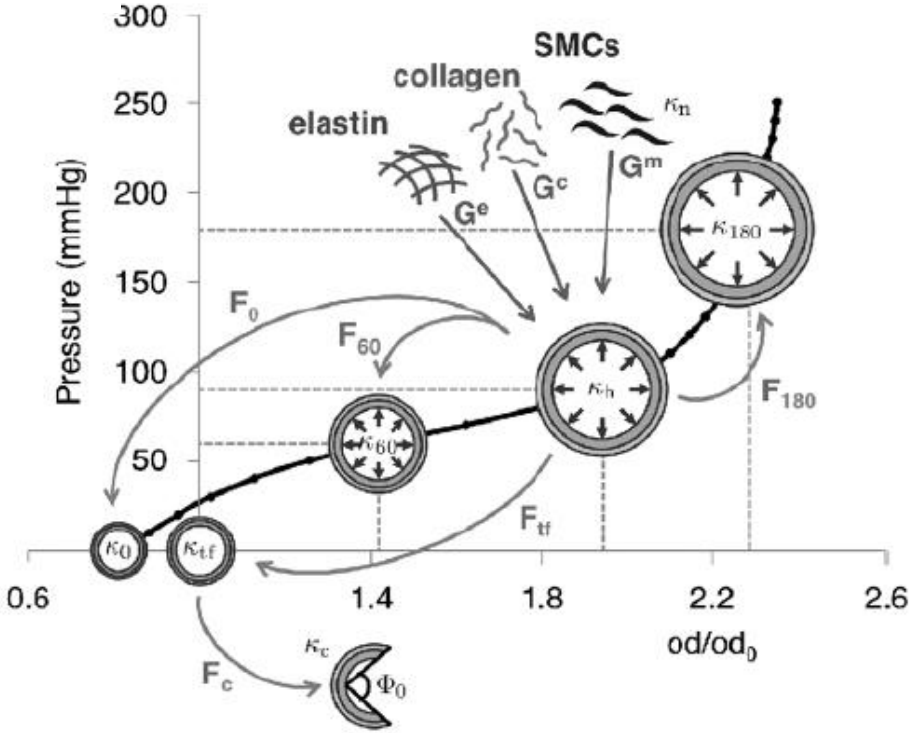

avril@emse.fr

APPROACH

1. Experiments
2. Material model
3. **Inverse method**

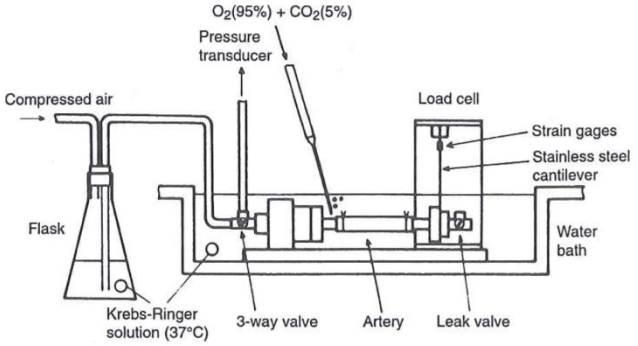

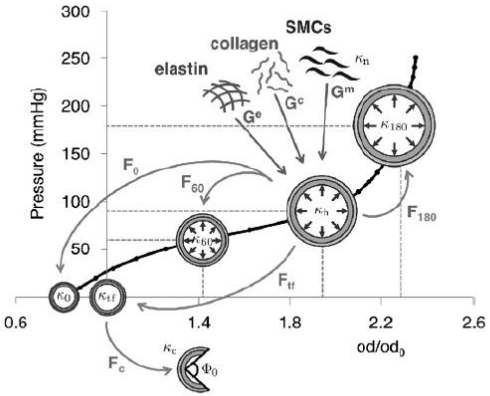

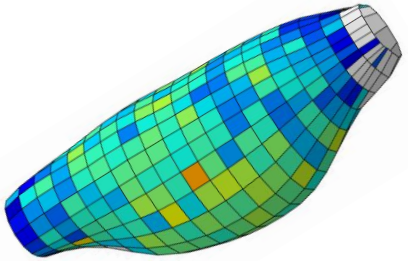

Inverse approach: the virtual fields method

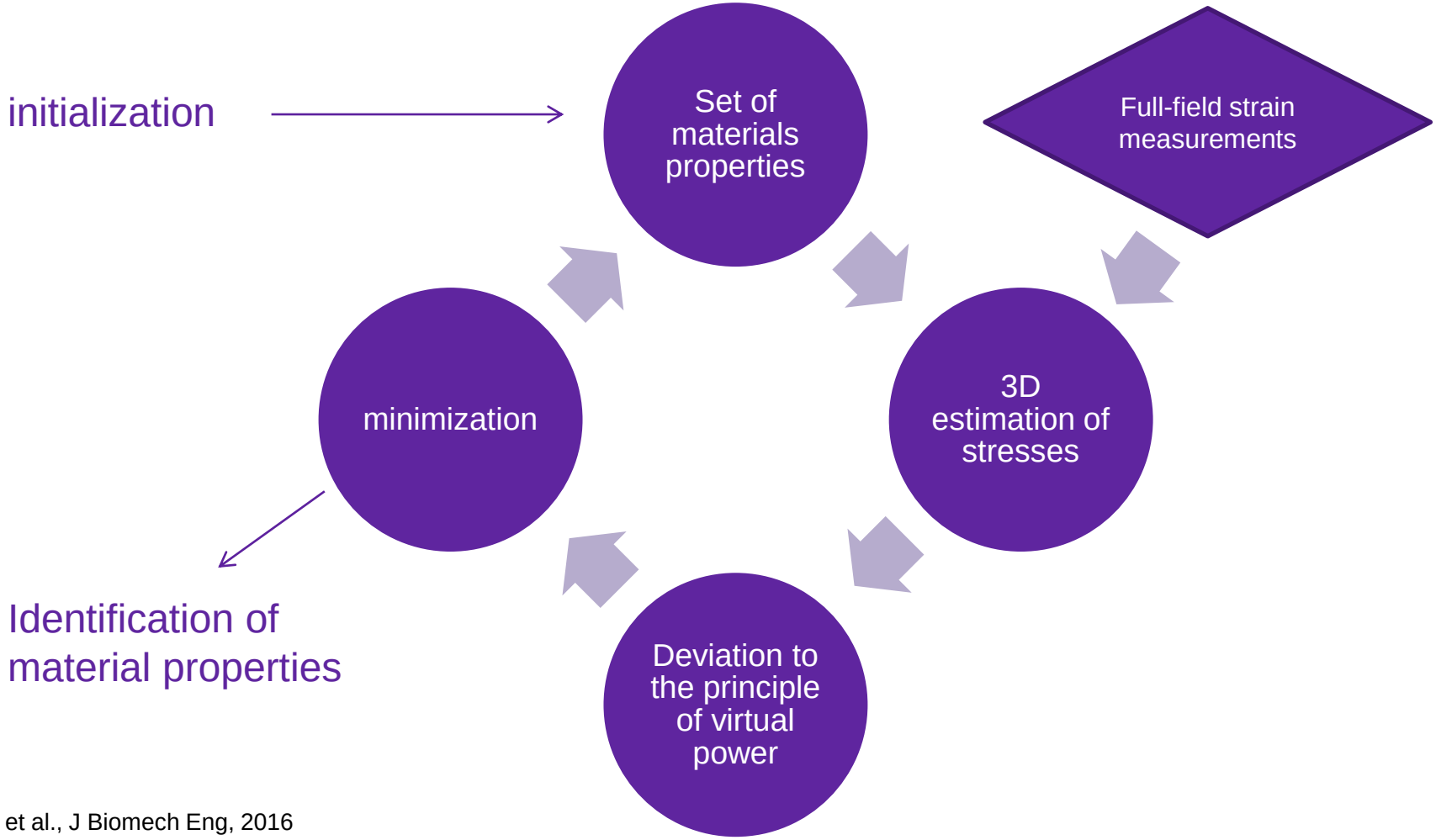

Bersi et al., J Biomech Eng, 2016

Full-field stress reconstruction

initialization →

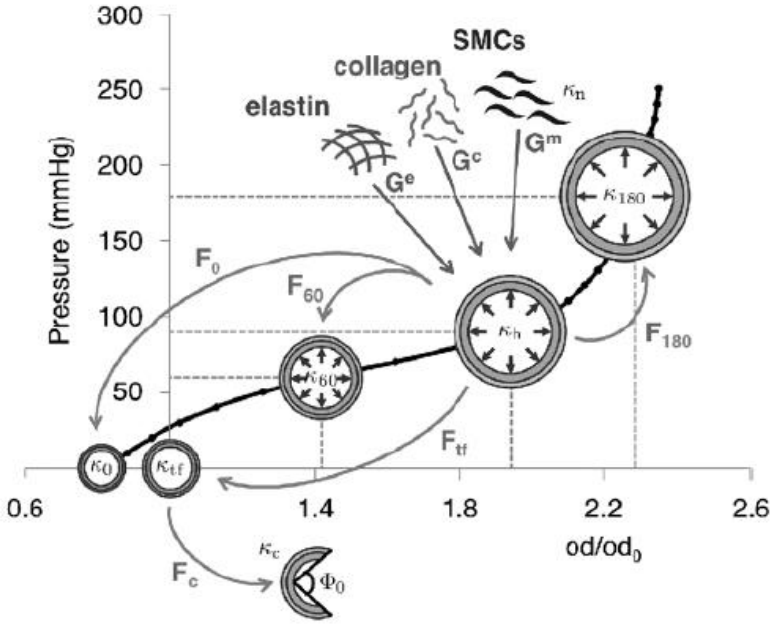

Set of materials properties

Full-field strain measurements

3D estimation of stresses

Simple application of the constitutive model for each element

Minimization of the equilibrium gap using the principle of virtual power

minimization

$$J = \sum_{p} \sum_{\lambda} \left(\underbrace{-\int_{\omega(t)} \underline{\underline{\sigma}} : \left(\underline{\nabla} \otimes \underline{\xi}^* \right) d\omega}_{P^*_{int}} + \underbrace{\oint_{\partial\omega(t)} \underline{T} \cdot \underline{\xi}^* \, ds}_{P^*_{ext}} \right)^2$$

Bersi et al., J Biomech Eng, 2016

Resolution:

$$\min_{c_3^1, c_3^{2,3}, c_3^4, \alpha, \beta} \left[\min_{c^e, c_2^1, c_2^{2,3}, c_2^4} \left[\frac{J(u)}{A} + \frac{J(v)}{B} \right] \right]$$

Linear least-squares

Genetic algorithm

Application to determine structure/function relationships in mice models of dissections

RESULTS

avril@emse.fr

3D stiffness reconstruction

Scientific Reports, 2020, 10(1), 1-23

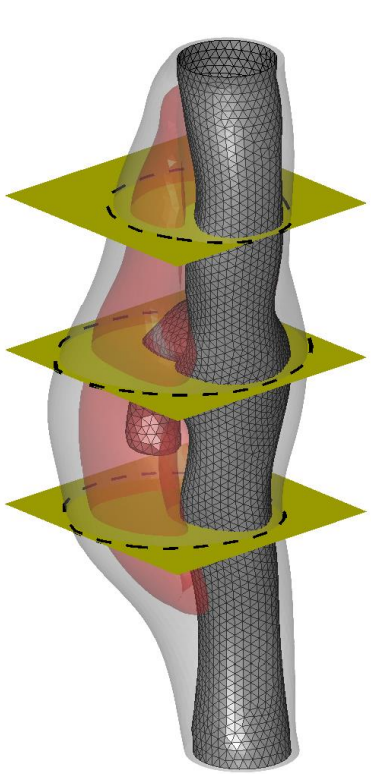

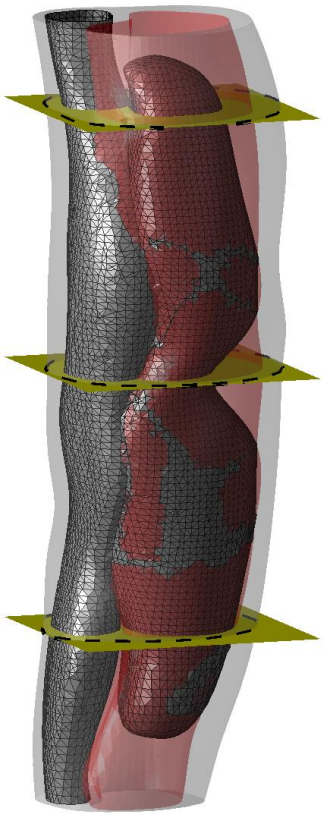

(kPa)

0 1000 2000 3000 4000

(kPa)

0 1000 2000 3000 4000

avril@emse.fr

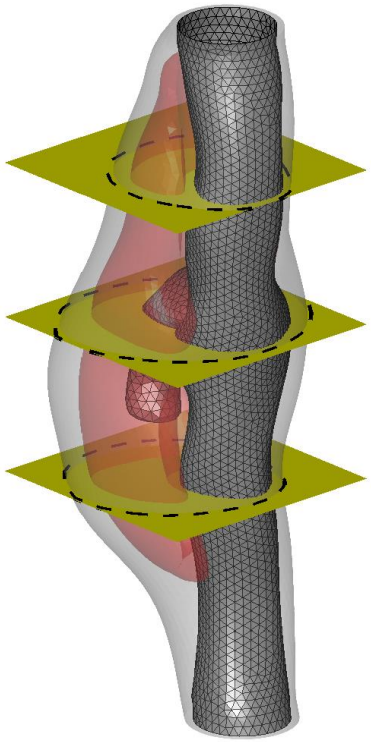

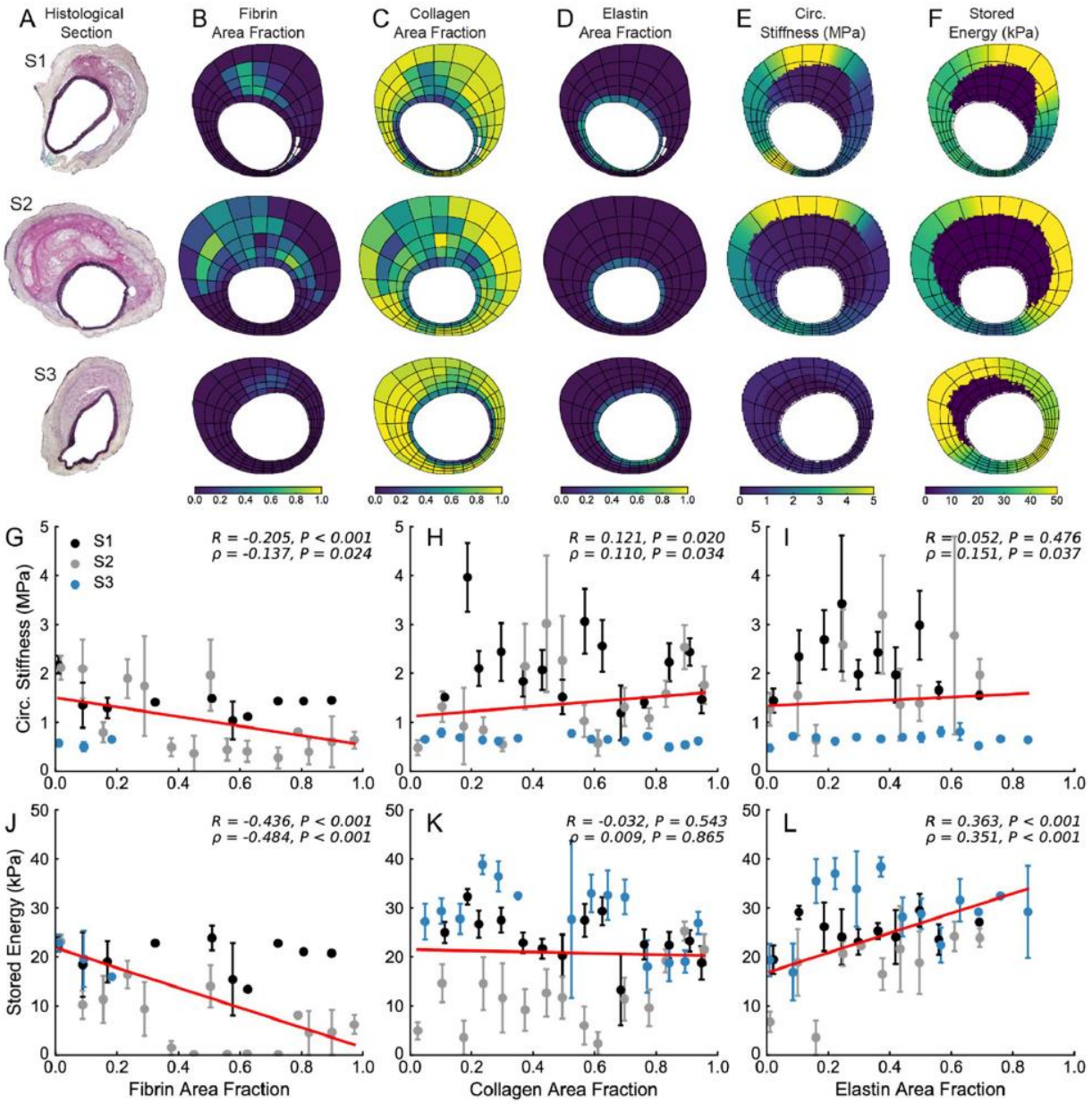
A Histological Section
B Fibrin Area Fraction
C Collagen Area Fraction
D Elastin Area Fraction
E Circ. Stiffness (MPa)
F Stored Energy (kPa)
S1
S2
S3
G
H
I
J
K
L
R = -0.205, P < 0.001
ρ = -0.137, P = 0.024
R = 0.121, P = 0.020
ρ = 0.110, P = 0.034
R = 0.052, P = 0.476
ρ = 0.151, P = 0.037
R = -0.436, P < 0.001
ρ = -0.484, P < 0.001
R = -0.032, P = 0.543
ρ = 0.009, P = 0.865
R = 0.363, P < 0.001
ρ = 0.351, P < 0.001
Circ. Stiffness (MPa)
Stored Energy (kPa)
Fibrin Area Fraction
Collagen Area Fraction
Elastin Area Fraction

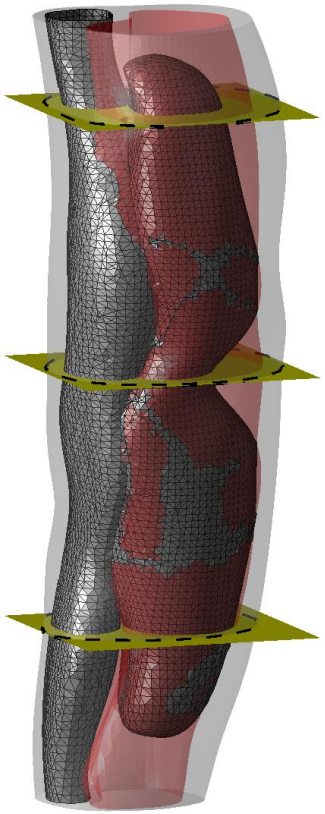

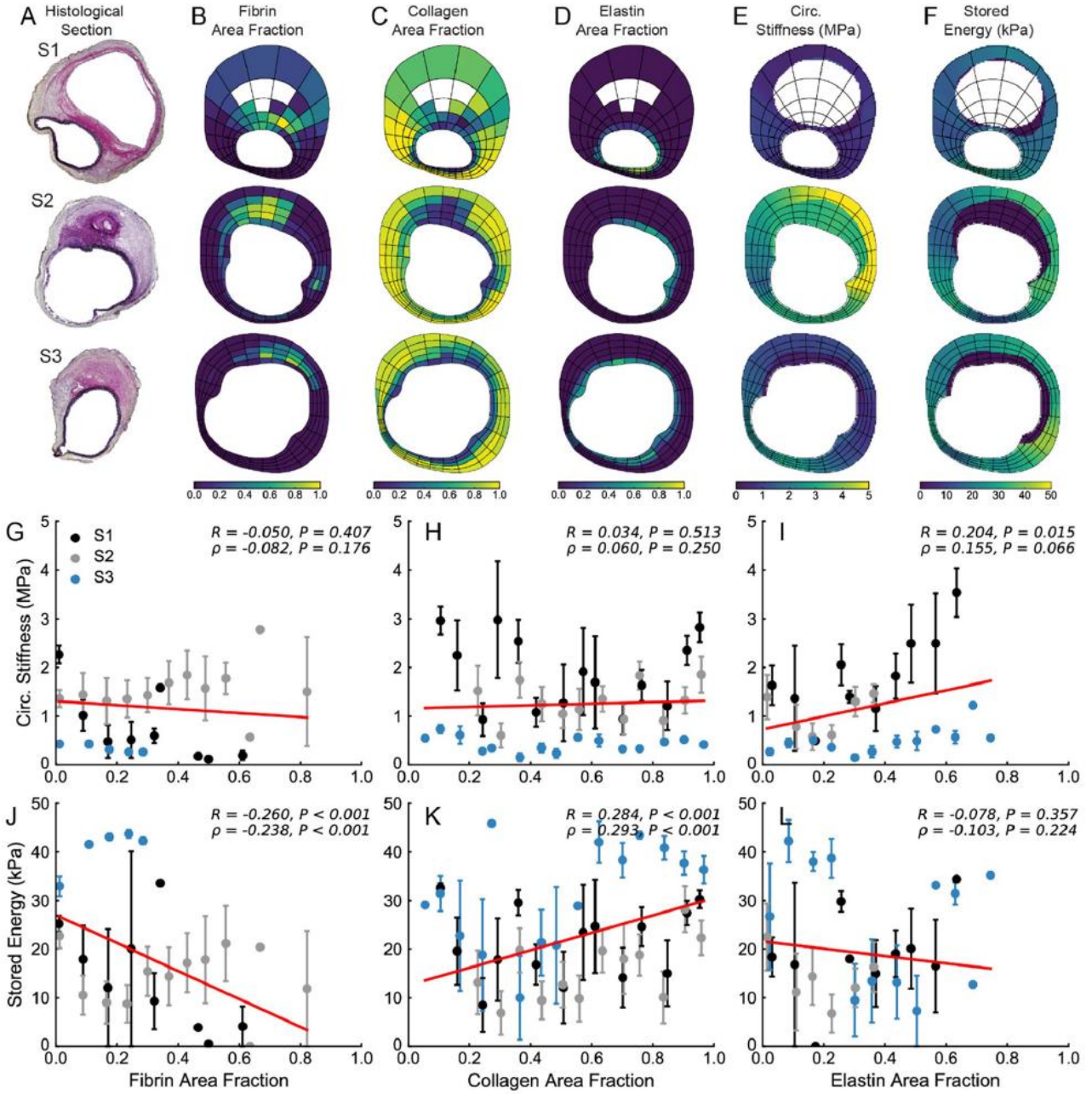

avril@emse.fr

Global correlation between microstructure and material properties

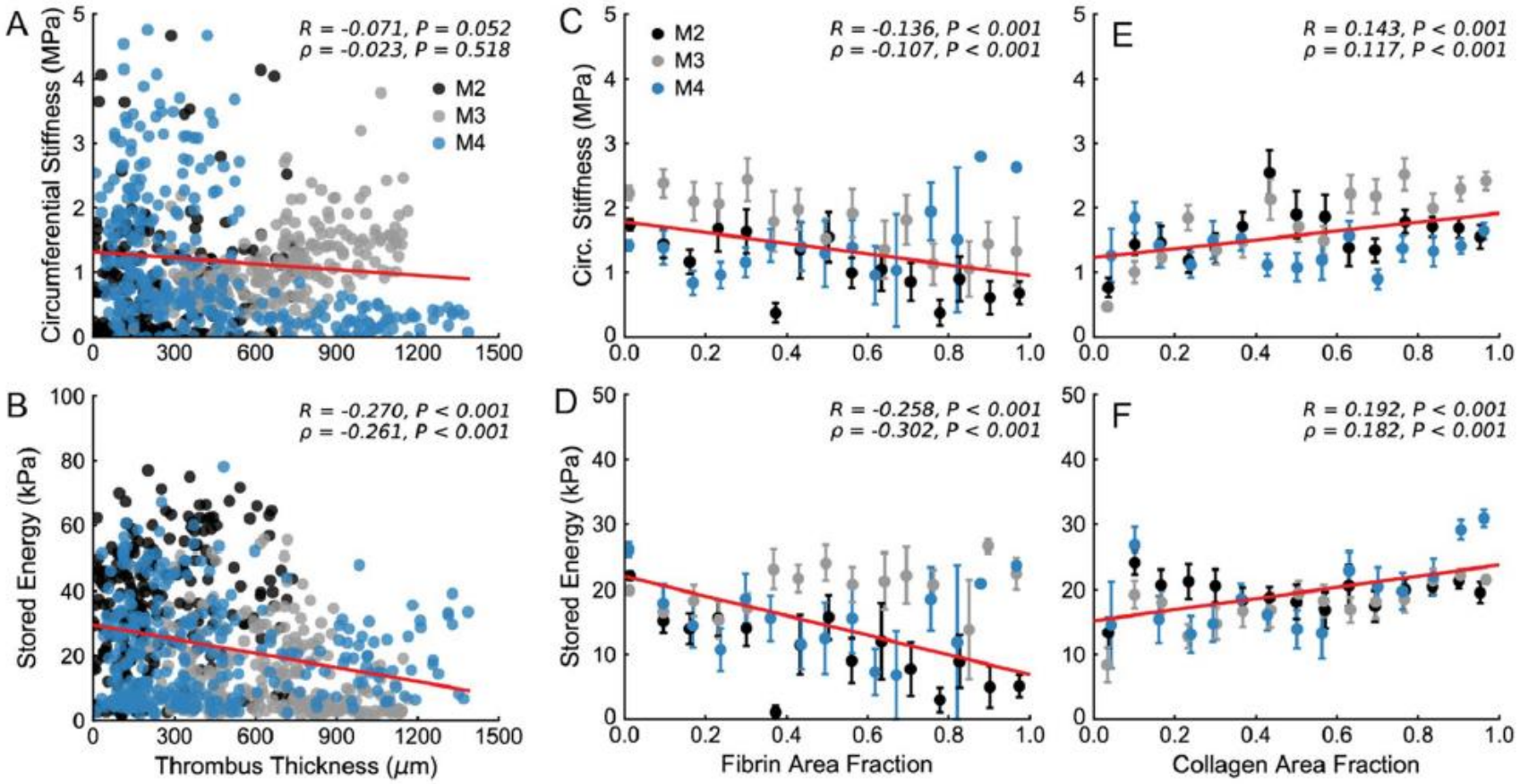

Scientific Reports, 2020, 10(1), 1-23

Local biomechanical dysfunction correlates with mural defects in the ATA

Weiss et al, ATVB, 2022

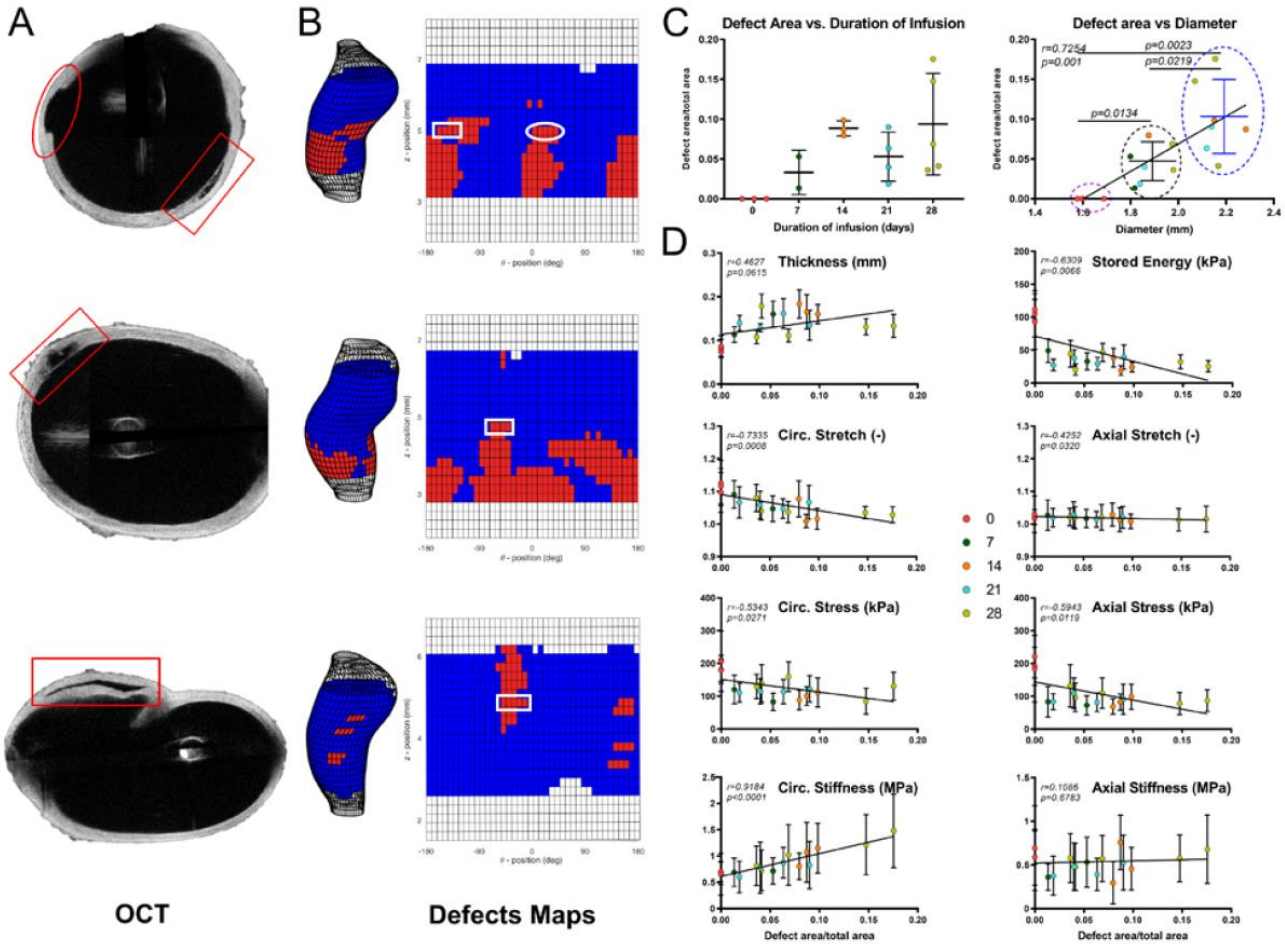

avril@emse.fr

SUMMARY

- Inverse approach permitting to reconstruct the **regional distribution of mechanical properties** of the aorta.

- Towards correlations between mechanical properties and underlying microstructures during aneurysm growth.

- 100 to 1000 independent local responses which could be used to set up **statistical mechanobiological models using Bayesian inference**.

What did we learn in terms of mechanobiology?

- Co-localization of mural composition, defects, and mechanical properties reveals marked biomechanical dysfunction of the aneurysmal wall

- Medial delaminations likely precede macroscopic defects (partial medial tears) due to redistributions of wall stress from damaged to initially undamaged tissue.

- Promoting robust collagen accumulation within regions of local mural degeneration protects the wall from catastrophic mechanical failure and should be pursued.

Acknowledgements

- Victor Acosta
- Brooks Lane
- Cristina Cavinato
- Chiara Bellini
- Matthew Bersi
- Dar Weiss
- Aaron Long
- Paolo Di Achille
- Katia Genovese
- Craig Goergen
- Jay Humphrey

Funding:
ERC-2014-CoG BIOLOCHANICS